U.S. DEPARTMENT OF ENERGY
JSA

Longitudinal target-spin asymmetries for deeply virtual Compton scattering at CLAS

Erin Seder

Irfu - CEA Saclay
Institut de recherche sur les lois fondamentales de l'Univers

Jefferson Lab
Thomas Jefferson National Accelerator Facility

Deeply Virtual Compton Scattering and Generalized Parton Distributions

$Q^2 = -(\mathbf{p}_e - \mathbf{p}_{e'})^2$ **Large, with** $Q^2 >> t = (\mathbf{p}_p - \mathbf{p}_{p'})^2$

and fixed $x_B = \dfrac{Q^2}{2M_p\nu}$, $\nu = (E_e - E_{e'})$

factorization:

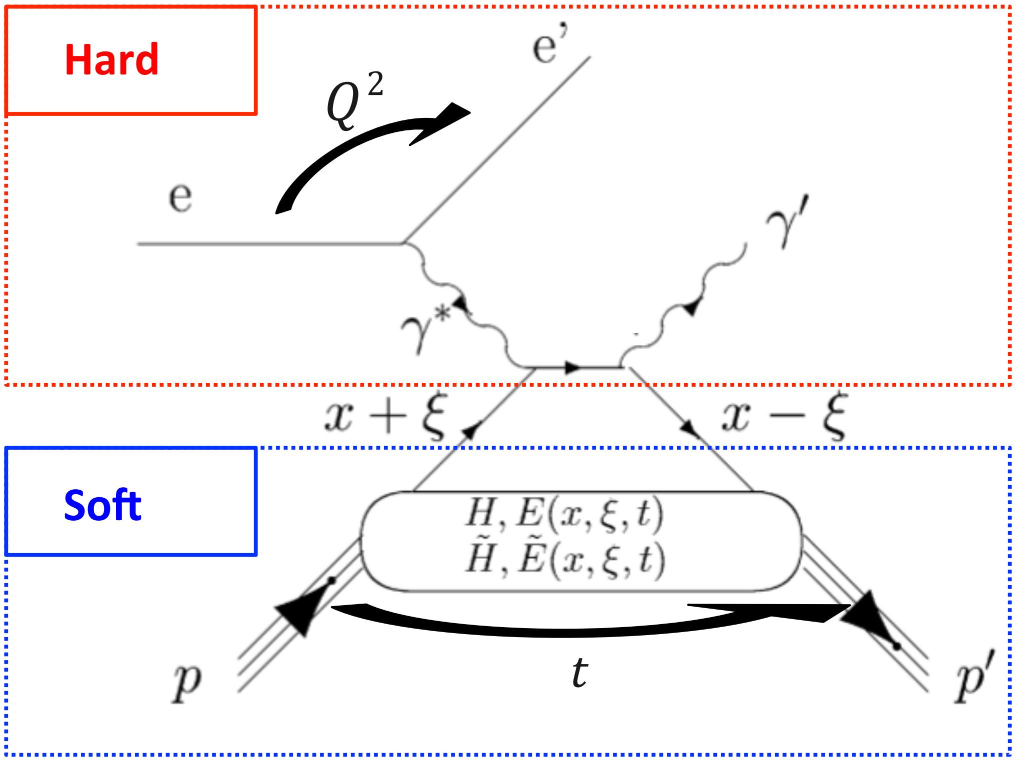

soft part described by 4 GPDs at LO

LO Generalized Parton Distributions (GPDs)

Vector: $\mathrm{H}(x,\xi,t)$, Axial-Vector: $\tilde{\mathrm{H}}(x,\xi,t)$

Tensor: $\mathrm{E}(x,\xi,t)$, Pseudoscalar: $\tilde{\mathrm{E}}(x,\xi,t)$

$x+\xi$
$x-\xi$: longitudinal quark momentum fraction

$$\xi \approx \frac{x_B}{2-x_B}$$

t : total squared momentum transfer to the nucleon

Generalized Parton Distributions

$$\mathrm{H}(x,\xi,t),\ \mathrm{E}(x,\xi,t)$$
$$\tilde{\mathrm{H}}(x,\xi,t),\ \tilde{\mathrm{E}}(x,\xi,t)$$

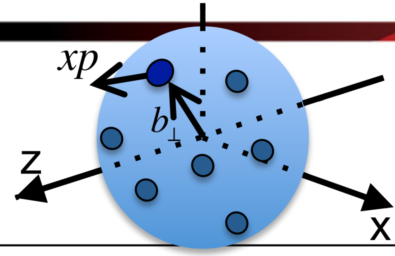

Fourier transform of the QCD non-local and non-diagonal operators

new information

Form Factors (FFs)

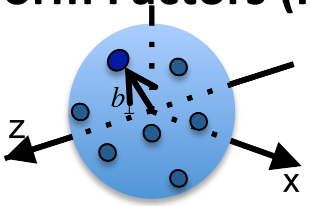

$$\int_{-1}^{1} dx\, \mathrm{H}^q(x,\xi,t) = F_1^q(t) \quad \text{Dirac}$$

$$\int_{-1}^{1} dx\, E^q(x,\xi,t) = F_2^q(t) \quad \text{Pauli}$$

$$\int_{-1}^{1} dx\, \tilde{\mathrm{H}}^q(x,\xi,t) = G_A^q(t) \quad \text{axial}$$

$$\int_{-1}^{1} dx\, \tilde{\mathrm{E}}^q(x,\xi,t) = G_p^q(t) \quad \text{pseudo-scalar}$$

Parton Distribution Functions (PDFs)

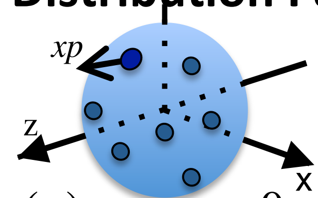

$$\mathrm{H}^q(x,0,0) = \begin{cases} q(x), & x>0 \\ -\bar{q}(-x), & x<0 \end{cases}$$

unpolarized quark distributions

$$\tilde{\mathrm{H}}^q(x,0,0) = \begin{cases} \Delta q(x), & x>0 \\ \Delta\bar{q}(-x), & x<0 \end{cases}$$

polarized quark distributions

Angular Momentum Sum Rule (X. Ji, Phy.Rev.Lett.78,610(1997))

$$J_q = \frac{1}{2}\int_{-1}^{1} dx\, x\,[\mathrm{H}^q(x,\xi,0) + E^q(x,\xi,0)]$$

Nucleon Tomography

(M. Burkardt, PRD 62, 71503(2000))

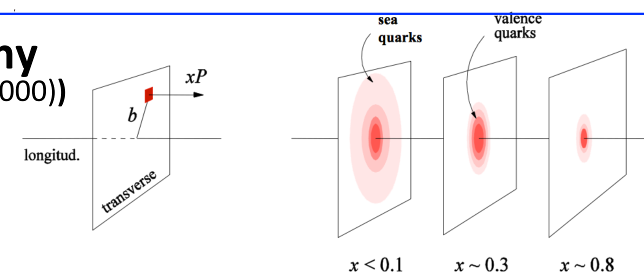

Accessing GPDs through DVCS

$$\frac{d\sigma}{dx_B dQ^2 d|t|\, d\phi} = \frac{x_B e^6 |\tau|^2}{32(2\pi^2)\sqrt{Q^2 + (2x_B M_p)^2}}$$

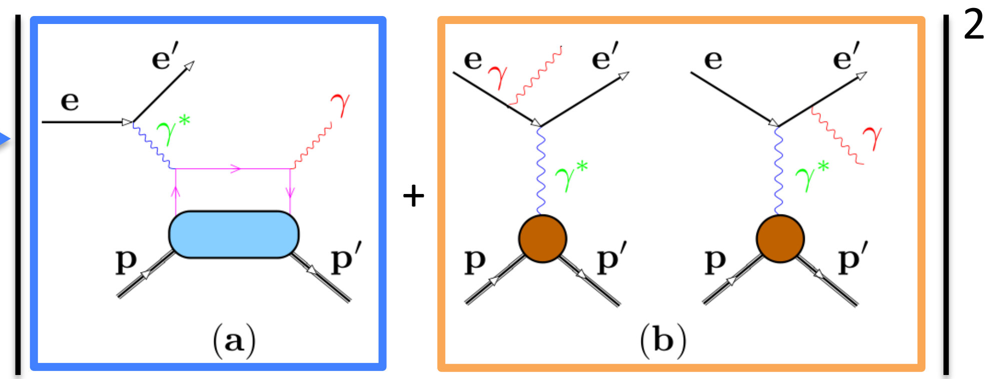

$$|\tau|^2 = |\tau_{BH}|^2 + |\tau_{DVCS}|^2 + |\tau_{DVCS}\tau^*_{BH} + \tau^*_{DVCS}\tau_{BH}|$$

τ_{BH} ➡ nucleon form factors F_1 and F_2

τ_{DVCS} ➡ $\int_{-1}^{1} \frac{H(x,\xi,t)}{x \pm \xi \mp i\varepsilon} dx + \ldots$ $|\tau_{DVCS}|^2$ ➡ bilinear combinations of GPDs

$I_{(DVCS \cdot BH)} = [\tau_{DVCS}\tau^*_{BH} + \tau^*_{DVCS}\tau_{BH}]$ ➡ linear combinations of GPDs

Accessing GPDs through DVCS

$$\frac{d\sigma}{dx_B dQ^2 d|t|\, d\phi} = \frac{x_B e^6 |\tau|^2}{32(2\pi^2)\sqrt{Q^2 + (2x_B M_p)^2}}$$

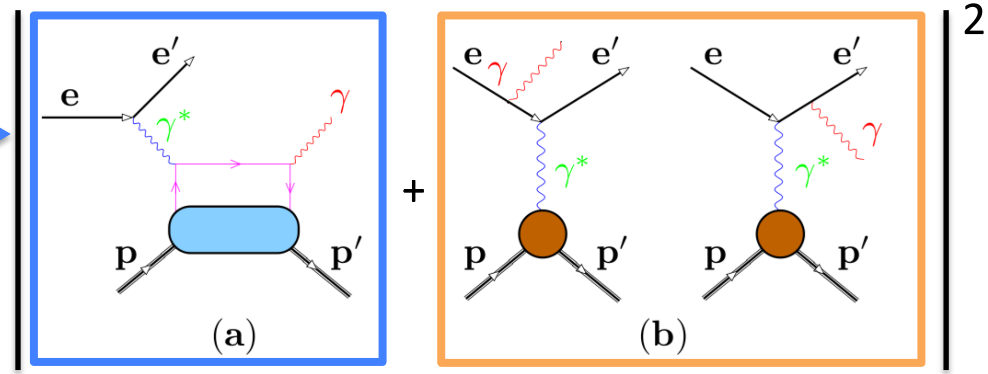

interference term, $I_{(\mathrm{DVCS \cdot BH})}$, can isolated via spin observables :

$$\Delta\sigma = \sigma^{\uparrow} - \sigma^{\downarrow} \sim I_{(DVCS \cdot BH)}$$

τ_{BH} ➡ nucleon form factors F_1 and F_2

τ_{DVCS} ➡ $\int_{-1}^{1} \frac{H(x,\xi,t)}{x \pm \xi \mp i\varepsilon} dx + \ldots$ $\quad |\tau_{DVCS}|^2$ ➡ bilinear combinations of GPDs

$I_{(DVCS \cdot BH)} = [\tau_{DVCS}\tau^{*}_{BH} + \tau^{*}_{DVCS}\tau_{BH}]$ ➡ linear combinations of GPDs

Accessing GPDs through DVCS

$$A = \frac{\Delta\sigma}{\sigma_{total}}$$

$$\tau_{DVCS} \sim \int_{-1}^{1} \frac{\mathrm{H}(x,\xi,t)}{x \pm \xi \mp i\varepsilon} dx + \ldots \;\;\Rightarrow\;\; \overbrace{P\int_{-1}^{1} \frac{\mathrm{H}(x,\xi,t)}{x \pm \xi} dx}^{\Re e\mathcal{H}} \overbrace{- i\pi \mathrm{H}(\pm\xi,\xi,t)}^{\Im m\mathcal{H}}$$

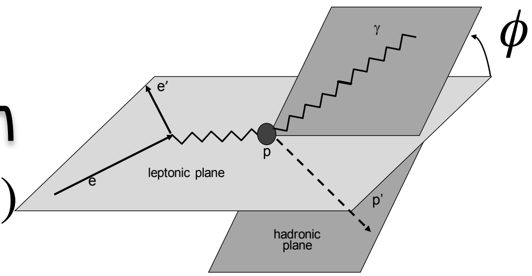

Polarized electron beam, unpolarized proton target (BSA):

$$\Delta\sigma_{LU} \sim \sin(\phi)\Im m\{F_1\mathcal{H} + \frac{x_B}{2 - x_B}(F_1 + F_2)\tilde{\mathcal{H}} - \frac{t}{4M^2}F_2\mathcal{E}\}d\phi \;\;\Rightarrow\;\; \Im m\{\mathcal{H}_p, \tilde{\mathcal{H}}_p, \mathcal{E}_p\}$$

Unpolarized electron beam, longitudinally polarized proton target (TSA) :

$$\Delta\sigma_{UL} \sim \sin(\phi)\Im m\{F_1\tilde{\mathcal{H}} + \frac{x_B}{2 - x_B}(F_1 + F_2)(\mathcal{H} + \frac{x_B}{2}\mathcal{E}) + \ldots\}d\phi \;\;\Rightarrow\;\; \Im m\{\tilde{\mathcal{H}}_p, \mathcal{H}_p\}$$

Polarized electron beam, longitudinally polarized proton target (DSA):

$$\Delta\sigma_{LL} \sim (A + B\cos(\phi))\Re e\{F_1\tilde{\mathcal{H}} + \frac{x_B}{2 - x_B}(F_1 + F_2)(\mathcal{H} + \frac{x_B}{2}\mathcal{E}) + \ldots\}d\phi \;\;\Rightarrow\;\; \Re e\{\mathcal{H}_p, \tilde{\mathcal{H}}_p\}$$

The more DVCS observables measured in the same kinematic regions = more constraints for GPD extraction.

Jefferson Lab & CLAS @ 6GeV

Continuous
Electron
Beam
Accelerator
Facility

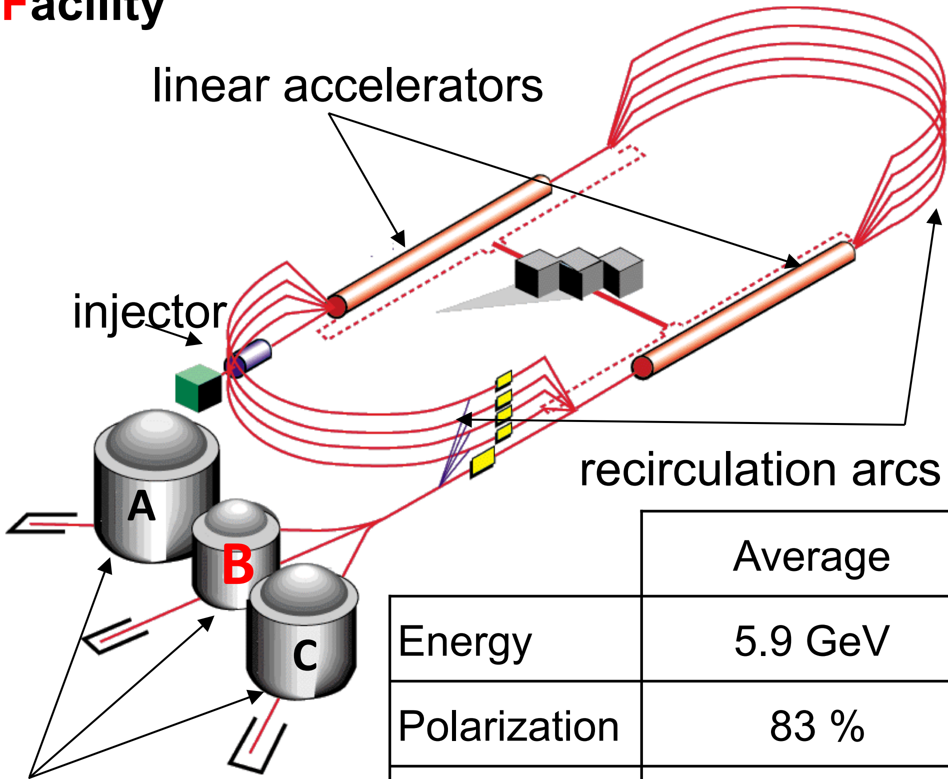

	Average
Energy	5.9 GeV
Polarization	83 %
Current to Hall-B	7.5 nA

CEBAF
Large
Acceptance
Spectrometer

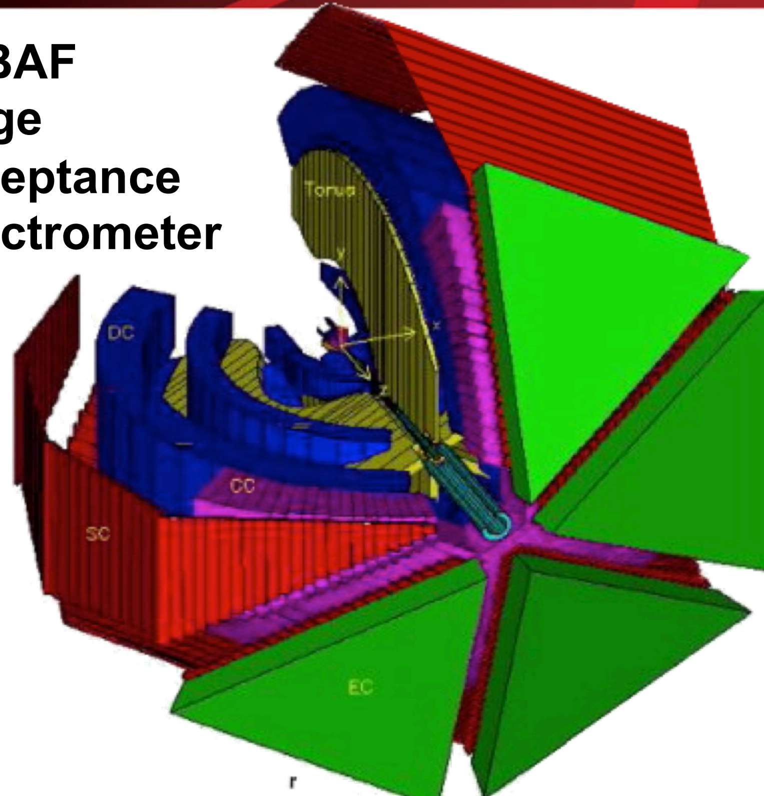

Toroidal Magnet (yellow)

- ➔ bends charged particles towards(away) from the beamline
- ➔splits the detector into 6 sectors in ϕ

Each sector:

- **3 segments of Drift Chambers (blue)**
- **Cerenkov Detectors (pink)**
- **Scintillation Counters (red)**
- **Electromagnetic Calorimeters (green)**

Previous CLAS DVCS Measurements

Non-dedicated experiment:

DVCS dedicated experiment:

Beam-spin asymmetry

S. Stepanyan et al., PRL 87 (2001).

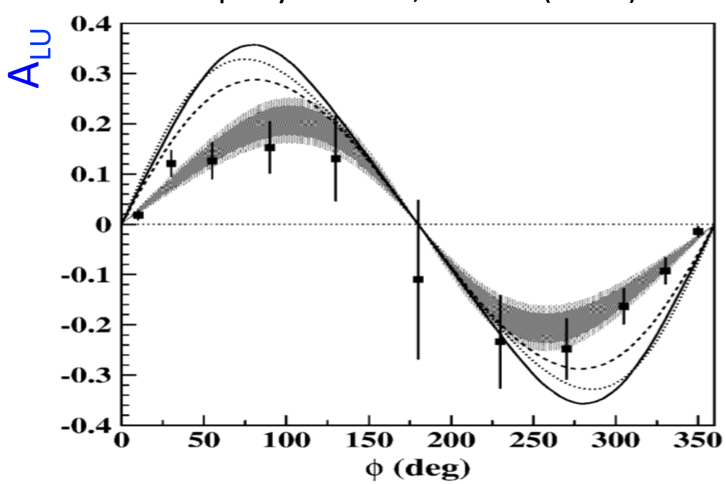

F.X. Girod et al., PRL 100 (2008).

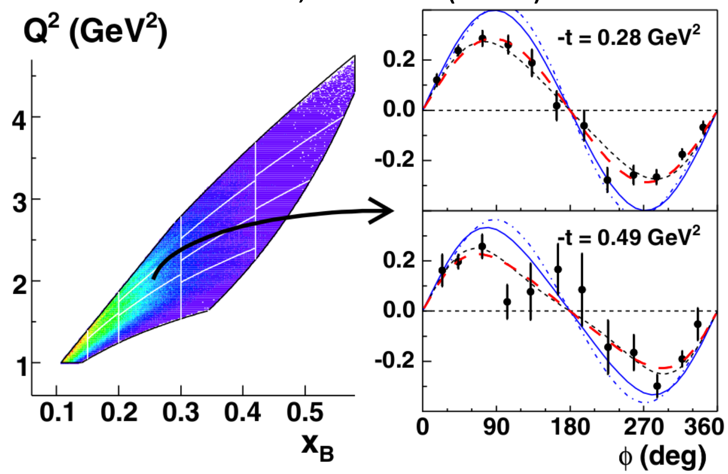

Target-spin asymmetry

S. Chen et al., PRL 97(2006).

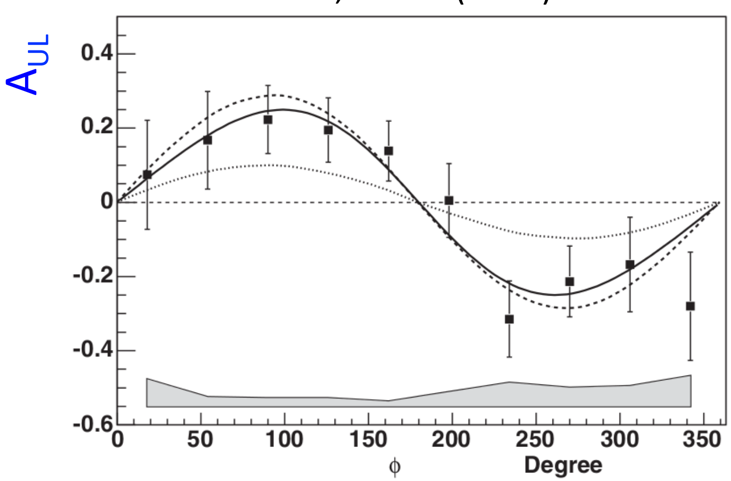

This Work

sufficient statistics for full 4-dimensional binning in kinematics:

Q^2, x_B, $-t$ and ϕ

EG1-DVCS CLAS Experiment

IC: Inner Calorimeter
increased coverage of low angle photons:

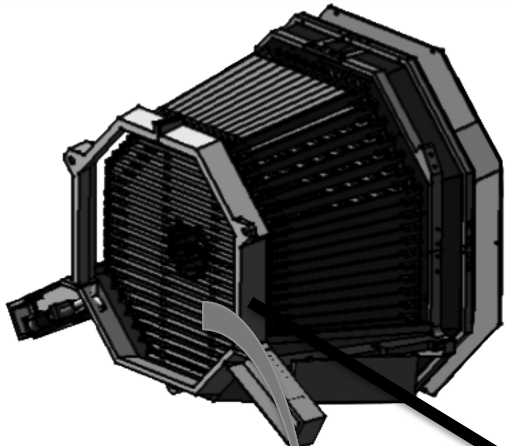

Photon coverage CLAS + IC

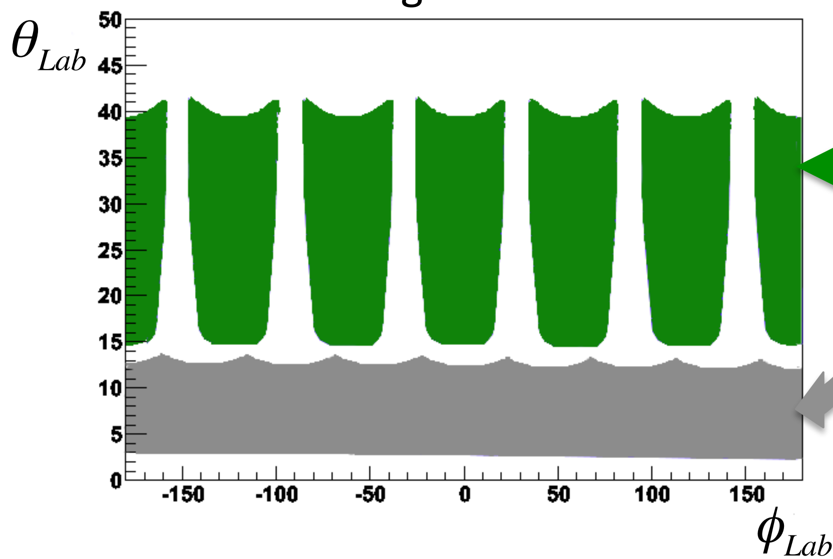

CEBAF
Large
Acceptance
Spectrometer

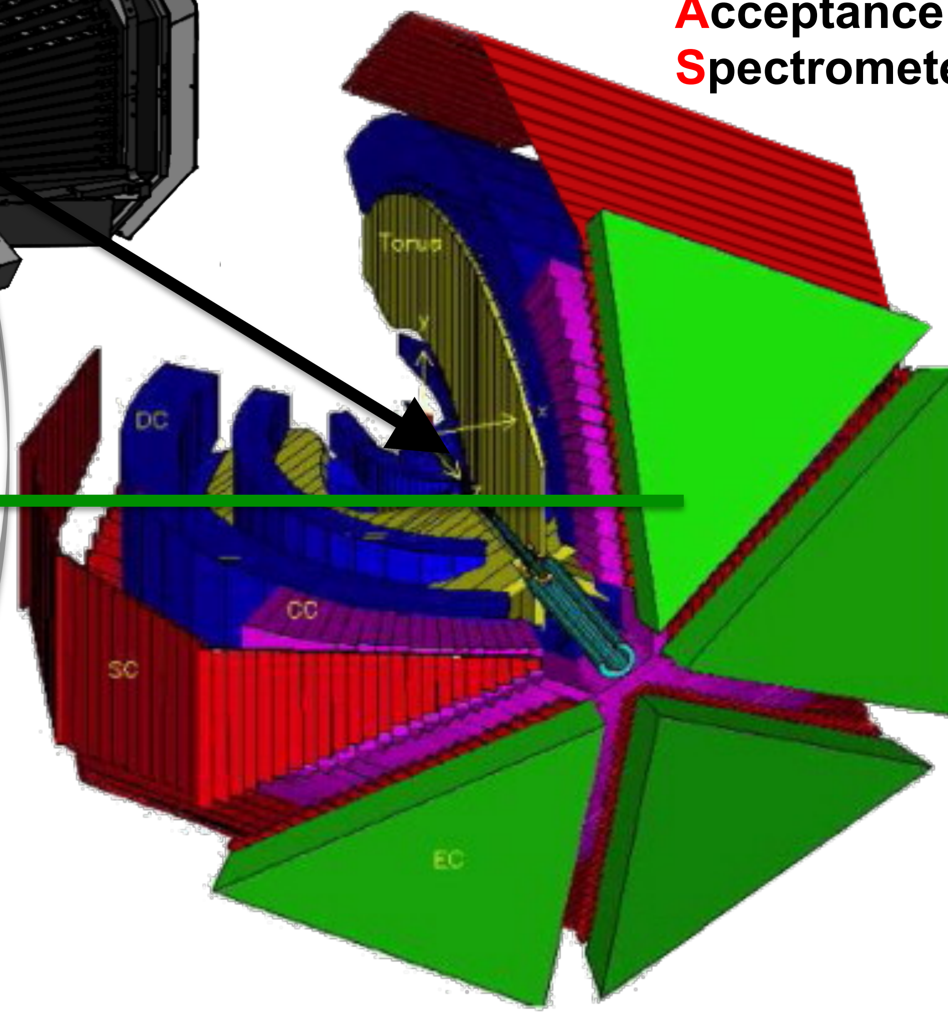

EG1-DVCS CLAS Experiment

Polarized Target

Solid beads of $^{14}NH_3$

Kept at 1 K

in a 5 T magnetic field

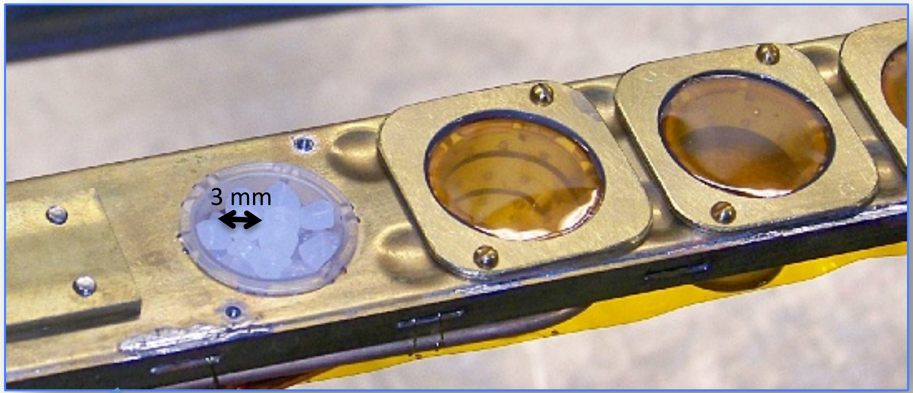

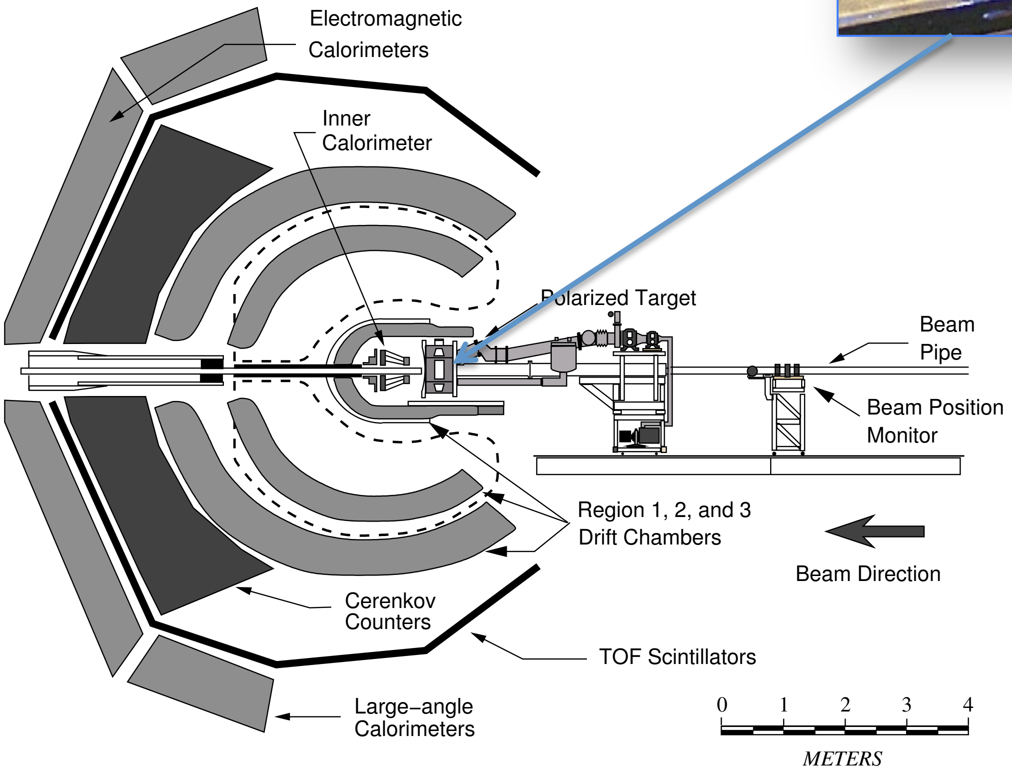

Continuously polarized via DNP

Average proton polarization ~79%

Event Selection $(ep \rightarrow e'p'\gamma)$

e'

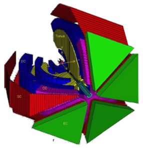

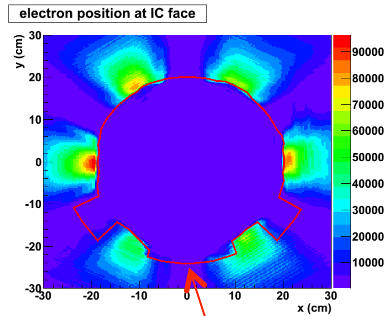

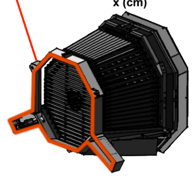

Negative Charge
Momentum > 0.8 GeV
| Vertex – Nominal | <= 3 cm
| timing difference CC – SC | <= 2ns
Energy deposited inner EC > 0.06 GeV
EC Fiducial cut
IC Shadow Cut

p'

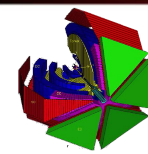

Positive Charge
| Vertex – Nominal | <= 4 cm
Momentum dependent β Cut
IC Shadow Cut

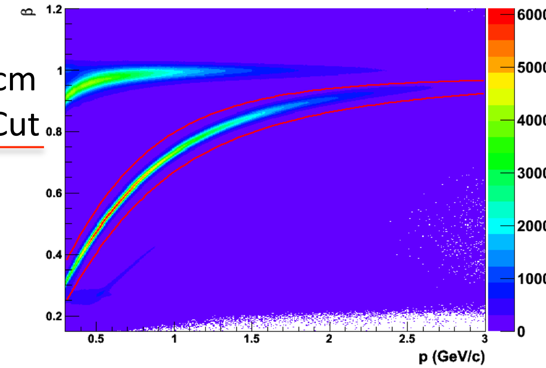

γ_{IC}

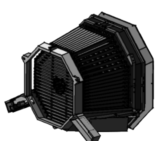

IC Fiducial cut

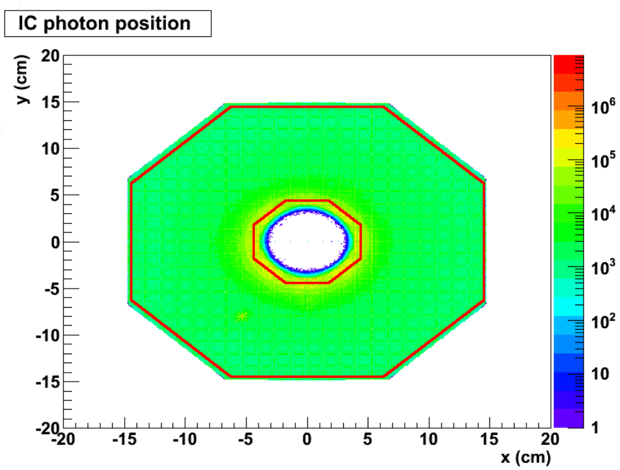

γ_{EC}

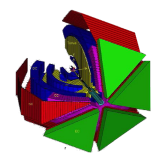

Neutral Charge
Energy > 0.25 GeV
β > 0.92
EC Fiducial cut
IC Shadow Cut

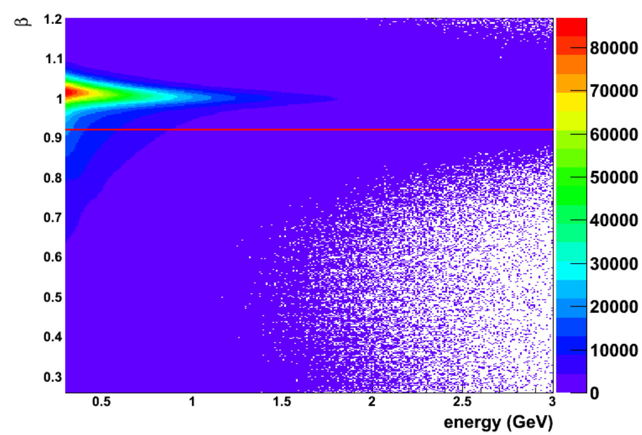

Event Selection $\left(ep \rightarrow e'p'\gamma\right)$

"Deep Inelastic Scattering" regime:

$Q^2 > 1\,(GeV/c)^2$ Momentum transfer squared of the electron

$W > 2\,GeV/c^2$ Mass of the system recoiling against the scattered electron

$E_\gamma > 1\,GeV \quad (Q^2 >> -t)$ detected photon energy

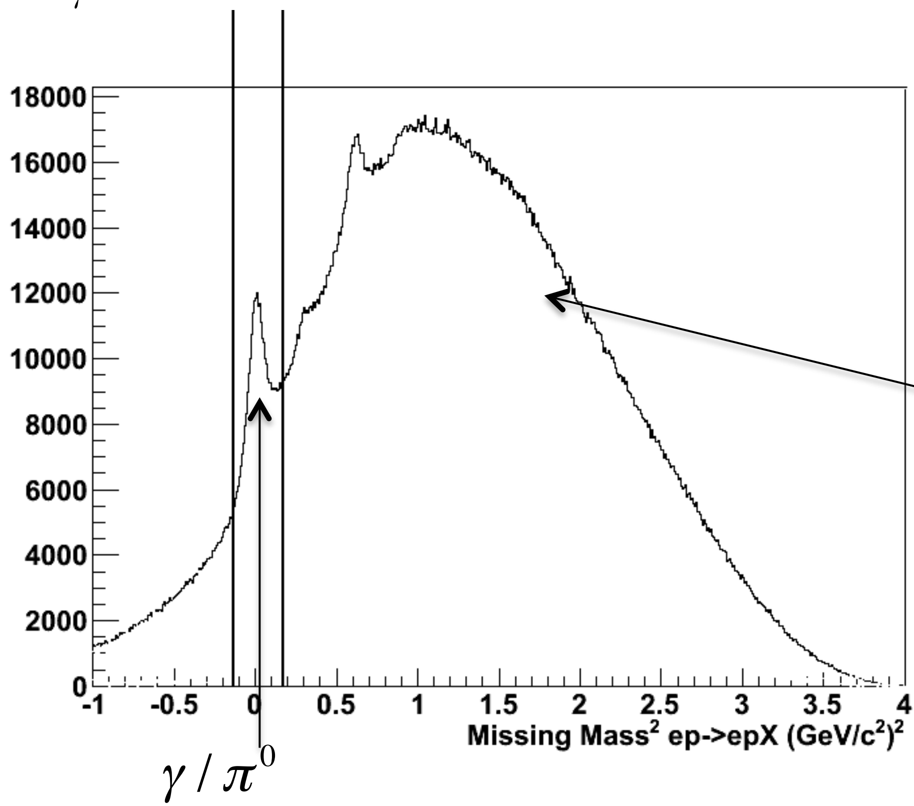

Missing mass squared of $ep \rightarrow ep\gamma$ of events with epγ detected

Large nuclear background estimate with carbon data

Event Selection $(ep \to e'p'\gamma)$

θ(γ-X) – angle between detected and expected photon

Δϕ – difference in calculated ϕ angle
1) using e, e', p’
2) using e, e', γ

pPerp – missing (x,y) momentum of ep->epγ

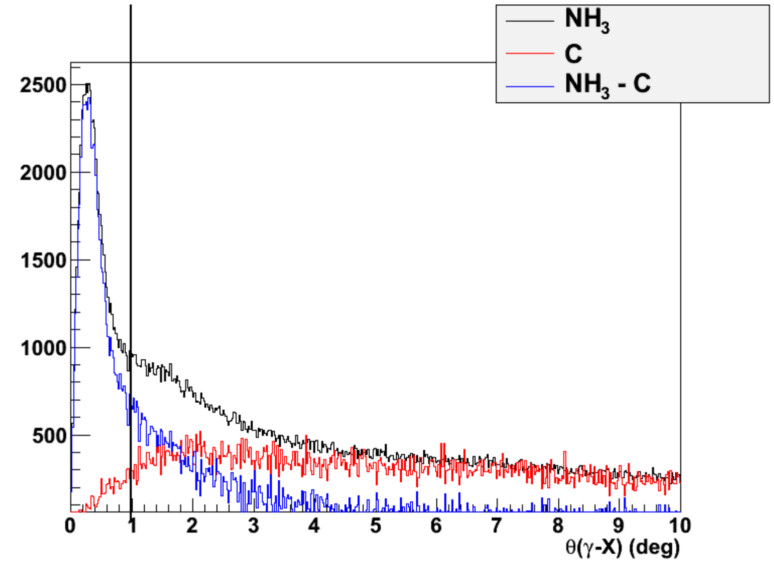

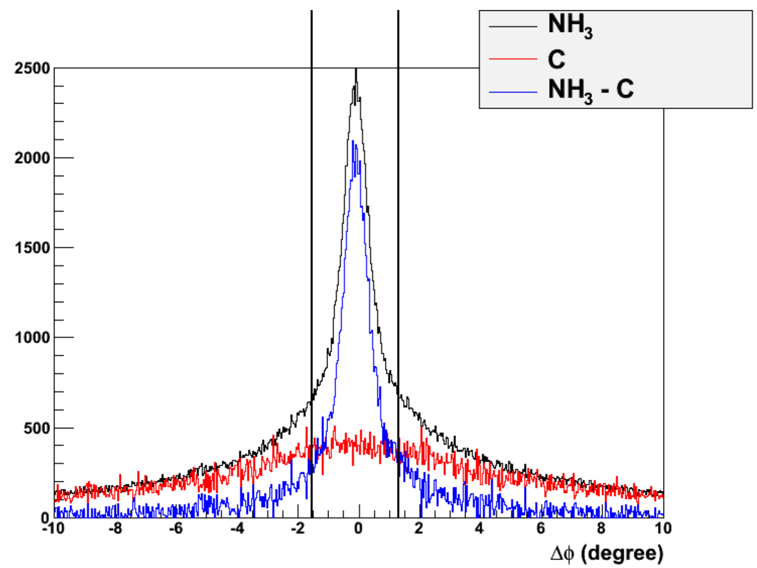

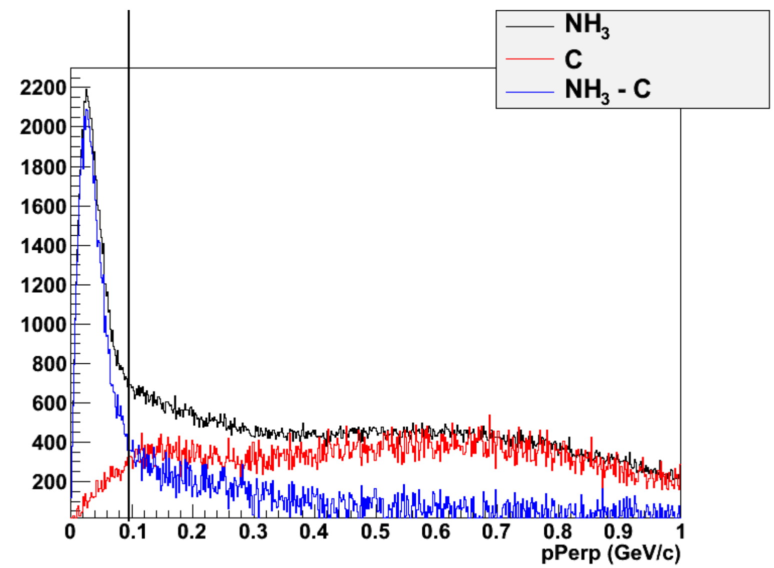

Nuclear Background

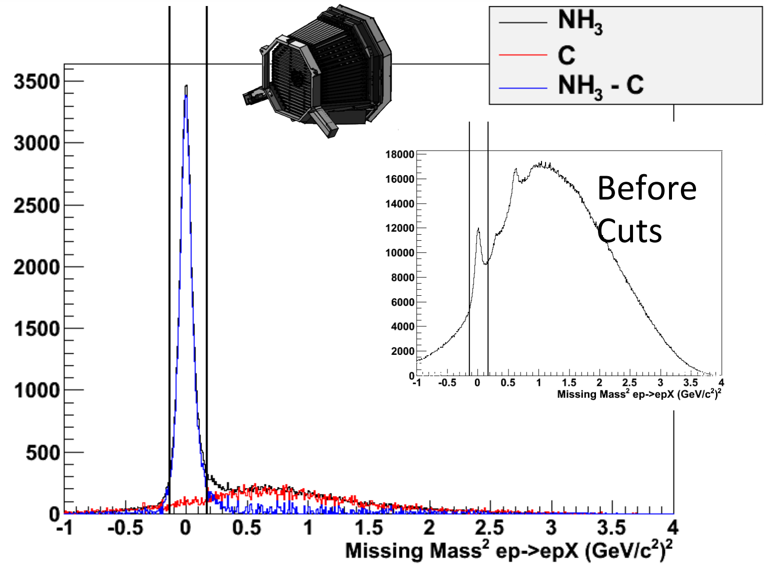

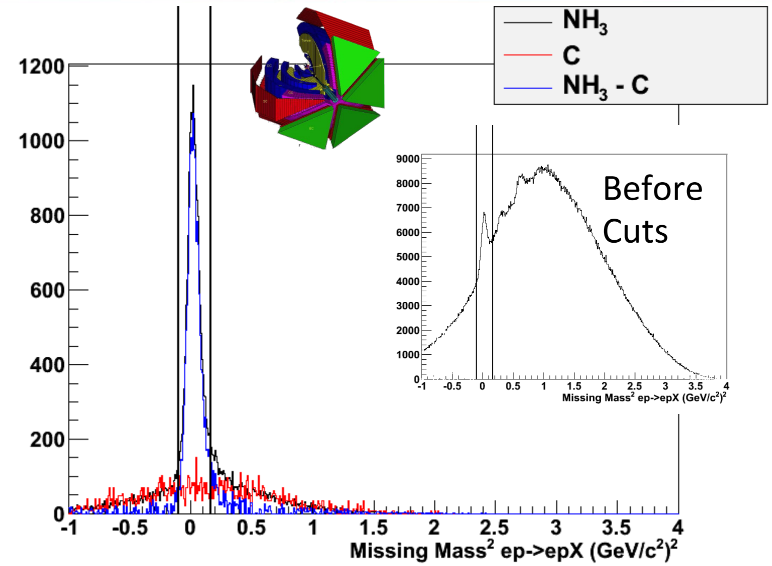

$$\boxed{D_f = 1 - \frac{N^{C}_{ep\gamma}}{N^{NH_3}_{ep\gamma}}}$$

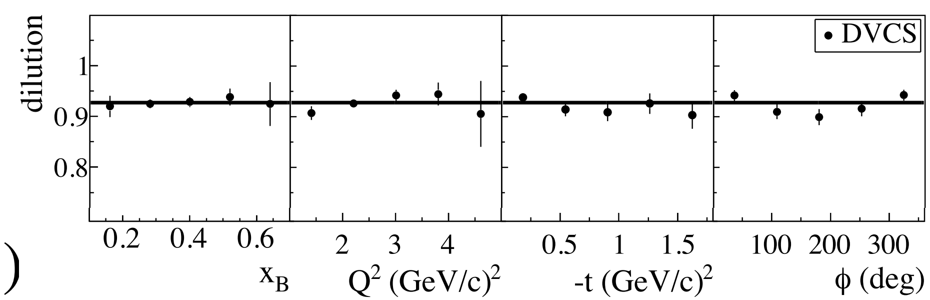

$$A_{UL} = \frac{1}{\boxed{D_f}} \frac{(N^{\downarrow\Uparrow} + N^{\uparrow\Uparrow}) - (N^{\downarrow\Downarrow} + N^{\uparrow\Downarrow})}{(N^{\downarrow\Uparrow} + N^{\uparrow\Uparrow})P^{\Downarrow} + (N^{\downarrow\Downarrow} + N^{\uparrow\Downarrow})P^{\Uparrow}}$$

electron helicity state

proton polarization state

Kinematic Binning

$$\boxed{Q^2} = -(\mathbf{p}_e - \mathbf{p}_{e'})^2, \quad \boxed{x_B} = \frac{Q^2}{2M_p(E_e - E_{e'})}$$

$$\boxed{t} = (\mathbf{p}_p - \mathbf{p}_{p'})^2$$

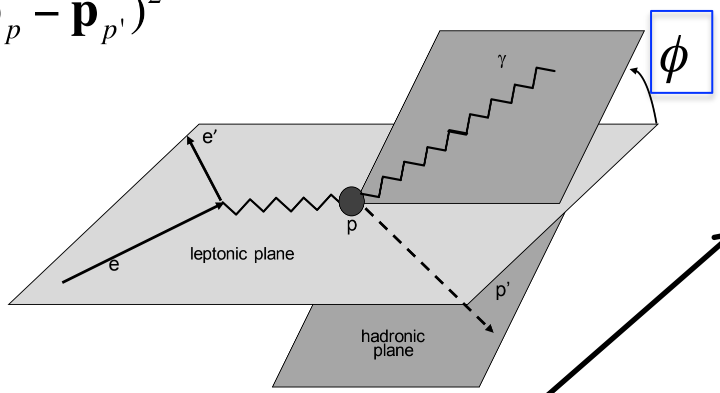

- 5 Bins in Q^2 x_B
- 4 Bins in -t
- 10 Bins in ϕ

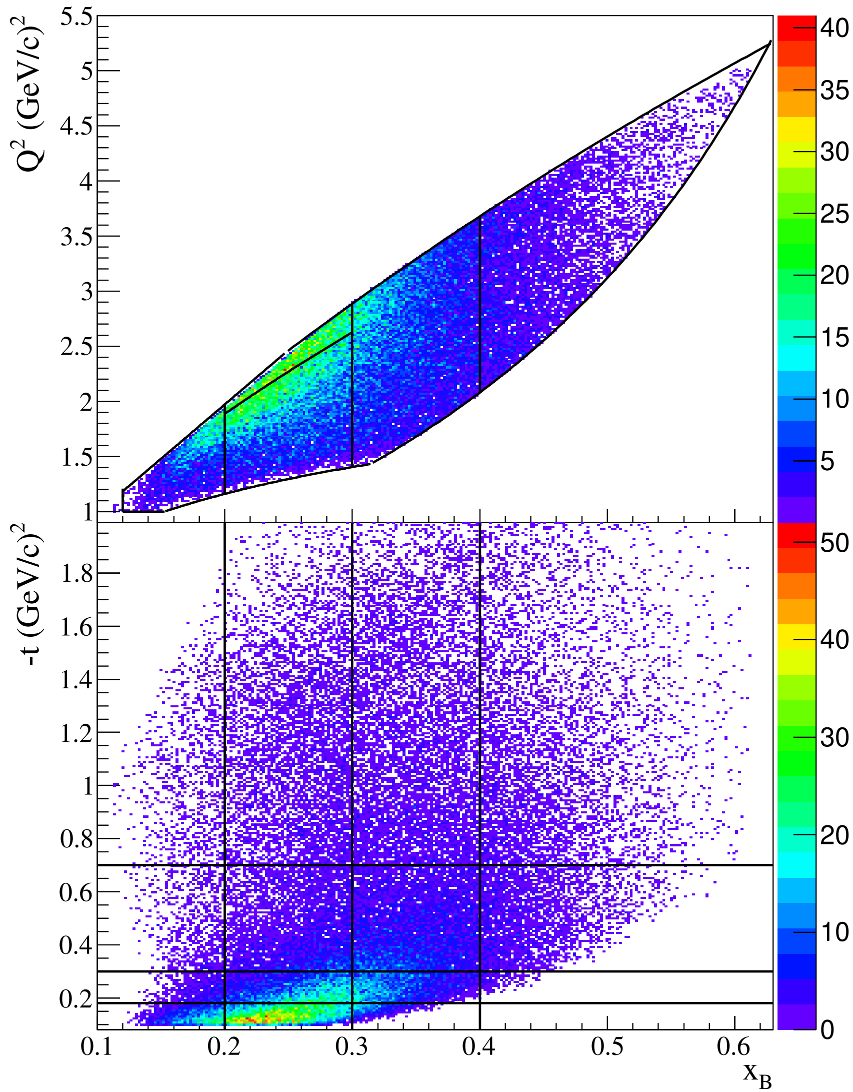

Jefferson Lab

π^0 Contamination

$$ep \rightarrow ep\pi^0 \rightarrow ep\gamma\gamma$$

➢π^0 electroproduction events where 1 of the π^0 decay photons has sufficiently high energy can reconstruct to appear as a single-photon electroproduction event

➢Event selection cuts reduce but not eliminate this contamination to single-photon events

➢The fraction of the epγ data which are actually epπ^0 events for each polarization configuration in each kinematic bin is estimated by the correction factor:

$$Bkgr_{\pi^0} = \left(\frac{N_{MC}^{ep\pi^0(\gamma)}}{N_{MC}^{ep\pi^0(\gamma\gamma)}}\right) * \left(\frac{N_{DATA}^{ep\pi^0}}{N_{DATA}^{ep\gamma}}\right) * \left(\frac{D_f^{ep\pi^0}}{D_f^{ep\gamma}}\right)$$

Acceptance ratio of single detected photon π^0 events in MC simulation

Ratio of epπ^0 to epγ events in data (scaled by respective nuclear background dilution factors)

The correction factor is applied on data as:

$$N^{\downarrow\Uparrow} = (1 - Bkgr_{\pi^0}^{\downarrow\Uparrow})\frac{N_{ep\gamma}^{\downarrow\Uparrow}}{FC^{\downarrow\Uparrow}}$$

π^0 Contamination

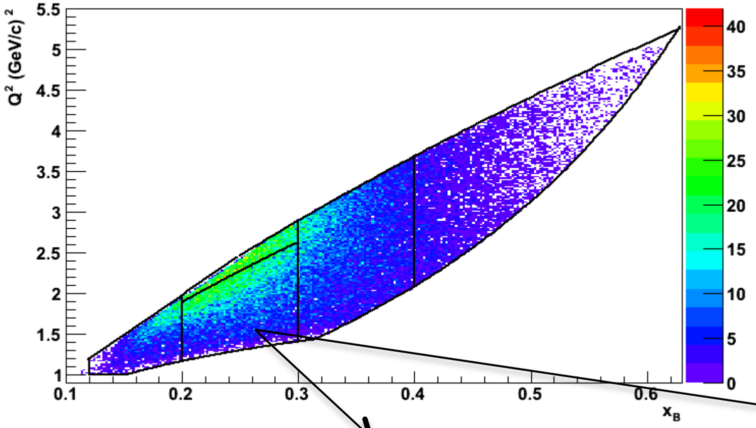

$$N^{\downarrow\Uparrow} = (1 - Bkgr_{\pi^0}^{\downarrow\Uparrow}) \frac{N_{ep\gamma}^{\downarrow\Uparrow}}{FC^{\downarrow\Uparrow}}$$

$$A_{UL} = \frac{1}{D_f} \frac{(N^{\downarrow\Uparrow} + N^{\uparrow\Uparrow}) - (N^{\downarrow\Downarrow} + N^{\uparrow\Downarrow})}{(N^{\downarrow\Uparrow} + N^{\uparrow\Uparrow})P^{\Downarrow} + (N^{\downarrow\Downarrow} + N^{\uparrow\Downarrow})P^{\Uparrow}}$$

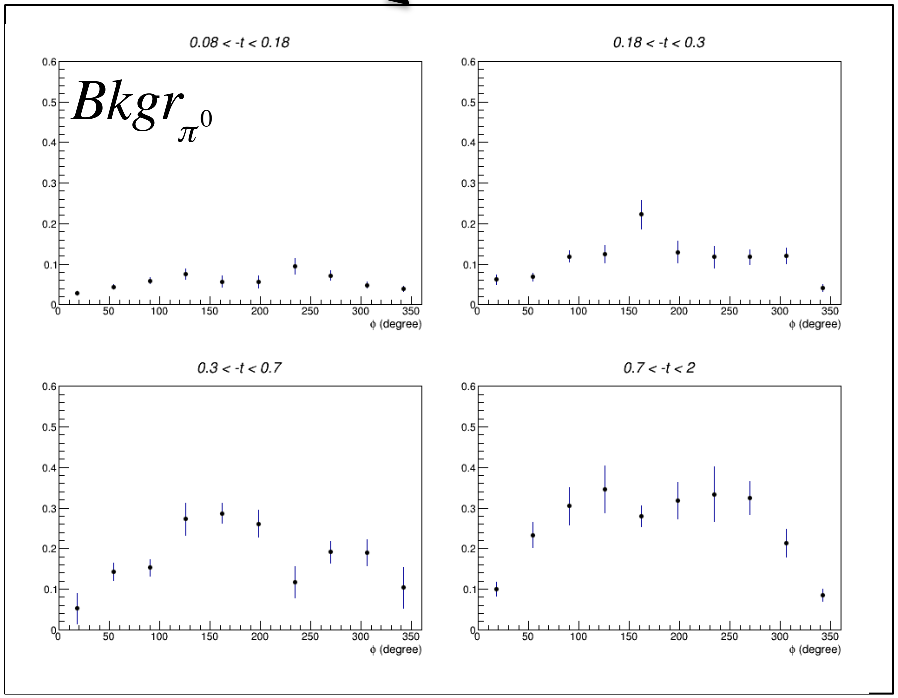

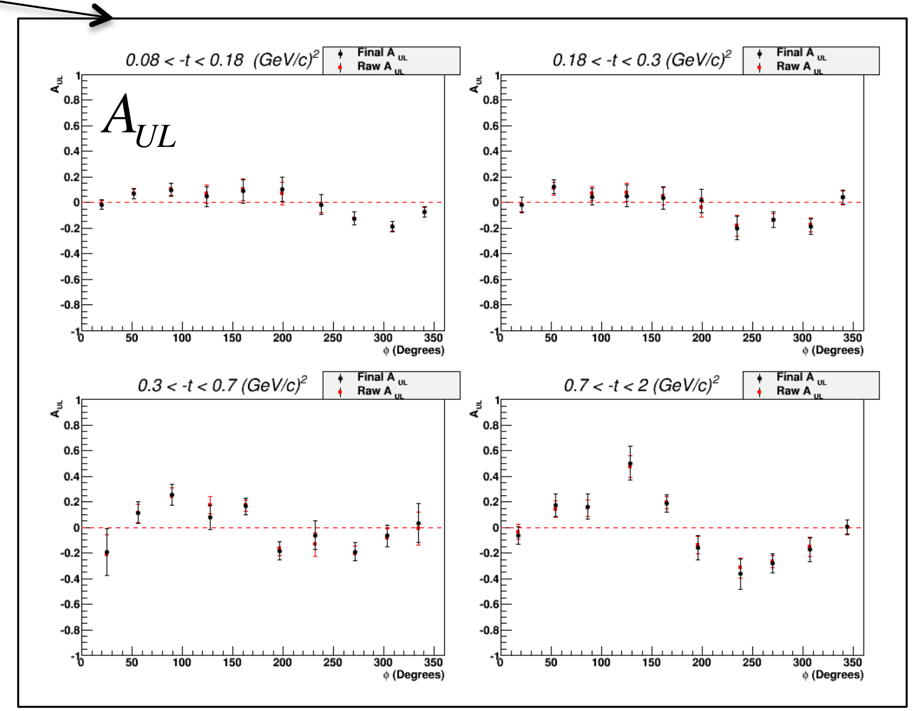

Proton Polarization

Through Elastic Scattering

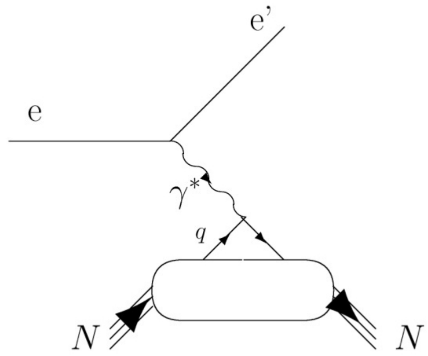

$$A_{meas} = \frac{1}{D_f}\frac{(N^{\downarrow\Uparrow} - N^{\uparrow\Uparrow})}{(N^{\downarrow\Uparrow} + N^{\uparrow\Uparrow})}$$

$$A_{meas} = (P_b P_t) A_{theory}$$

$\uparrow / \downarrow$ Electron Helicity State

$\Uparrow / \Downarrow$ Proton Polarization State

$$Q^2 > 1\,(GeV/c)^2$$

$$0.858 < W < 1.018\,(GeV/c^2)$$

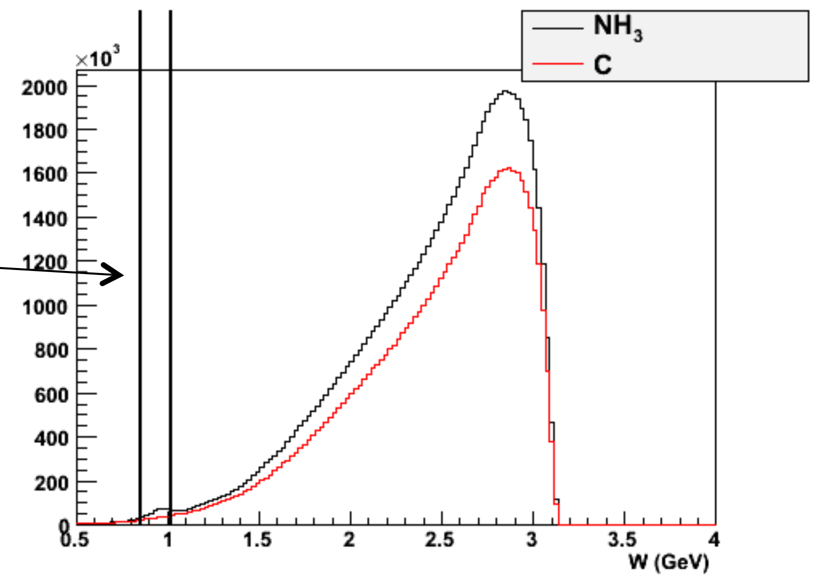

$$A_{UL} = \frac{1}{D_f}\frac{(N^{\downarrow\Uparrow} + N^{\uparrow\Uparrow}) - (N^{\downarrow\Downarrow} + N^{\uparrow\Downarrow})}{(N^{\downarrow\Uparrow} + N^{\uparrow\Uparrow})P^{\Downarrow} + (N^{\downarrow\Downarrow} + N^{\uparrow\Downarrow})P^{\Uparrow}}$$

Proton Polarization

Through Elastic Scattering

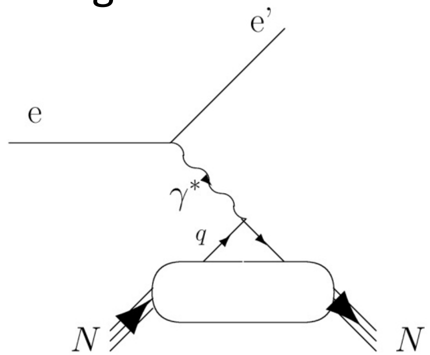

$$A_{meas} = \frac{1}{D_f}\frac{(N^{\downarrow\Uparrow} - N^{\uparrow\Uparrow})}{(N^{\downarrow\Uparrow} + N^{\uparrow\Uparrow})}$$

$$A_{meas} = (P_b P_t) A_{theory}$$

$\uparrow / \downarrow$ Electron Helicity State

$\Uparrow / \Downarrow$ Proton Polarization State

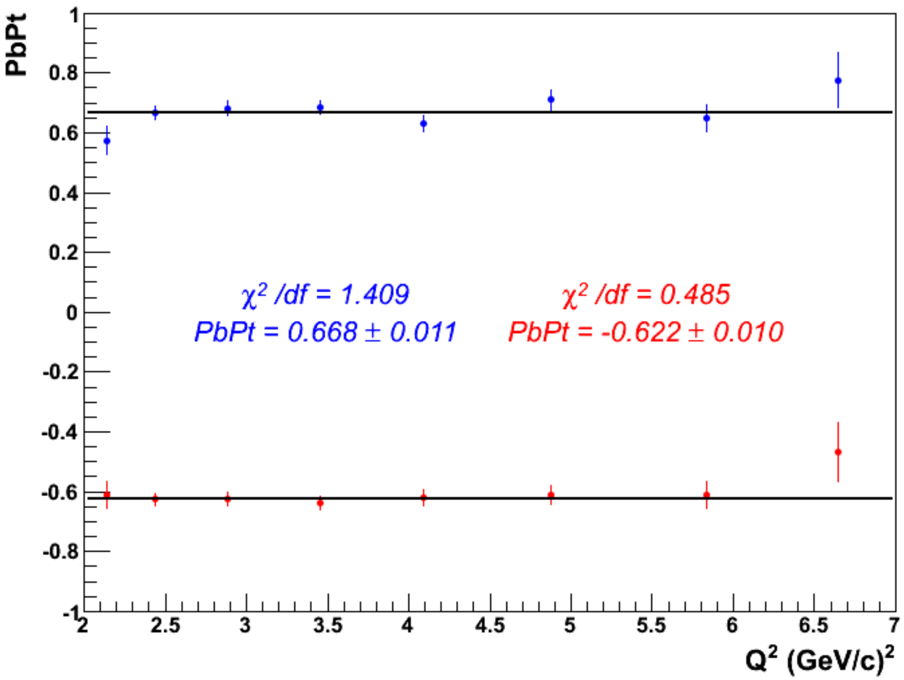

P_b – weighted average of Moller measurements ~ 0.83 (0.02)

	elastic (systematic error)	NMR
$P_t^{\Uparrow}$	80 (4)%	78%
$P_t^{\Downarrow}$	-74 (4)%	-77%

Transverse Corrections

What we measure and call longitudinal asymmetry is actually, when considered from the virtual- photon perspective, a combination of longitudinal and transverse asymmetries

Applied a model-dependent correction to obtain the TSA and DSA with respect to the virtual photon direction using the relationship[1]:

$$A_{UL}^{\gamma^*} = \frac{A_{UL}}{\cos\theta^*} + \tan\theta^* A_{UT}^{\gamma^*}(\phi_s = 0)$$

The angle formed by the virtual photon and the beam direction

The x-component of the transverse asymmetry (estimated with VGG)

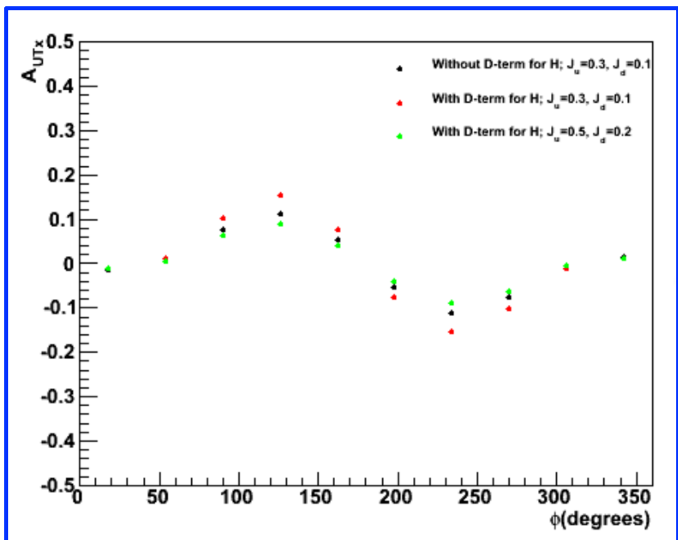

$\langle Q^2\rangle$ =1.97 GeV^2 ,$\langle x_B\rangle$ = 0.256

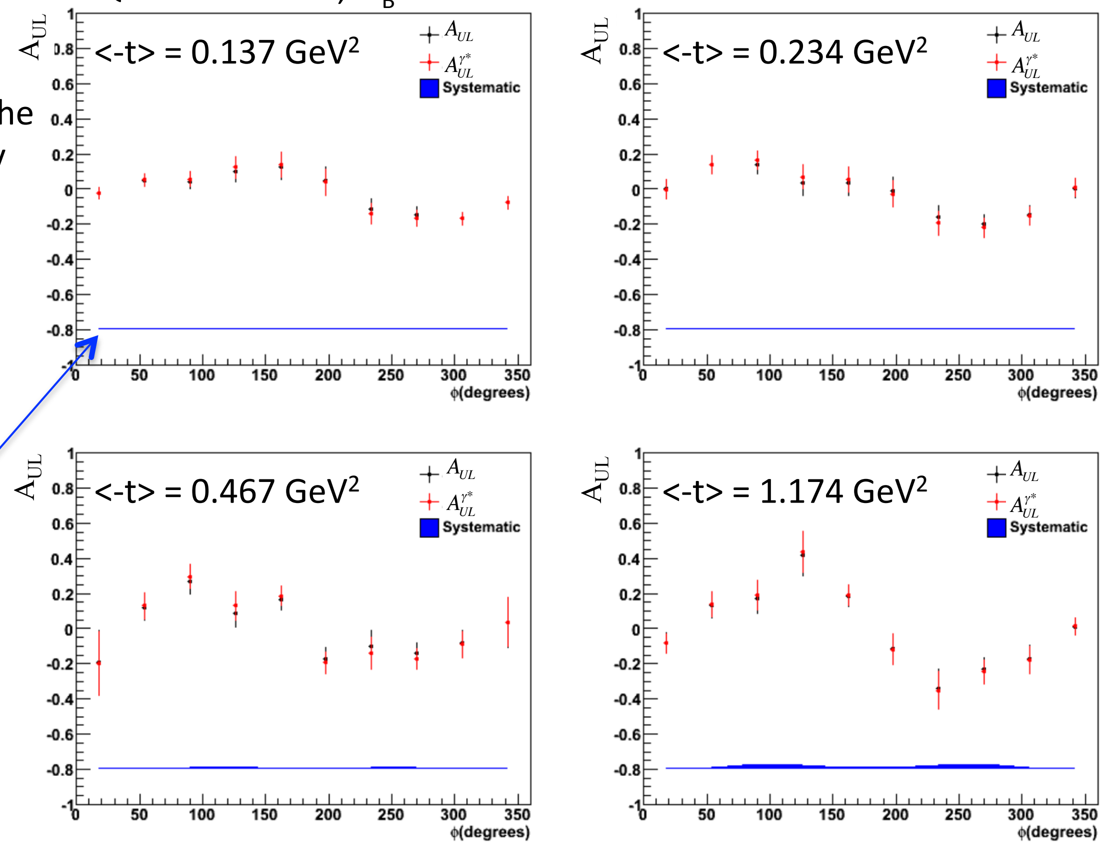

[1] M. Diehl and S. Sapeta, Eur. Phys. J. C41, 515 (2005).

Systematics

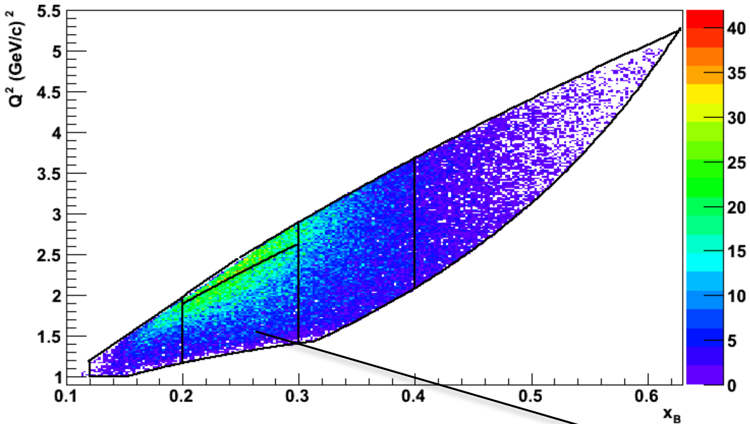

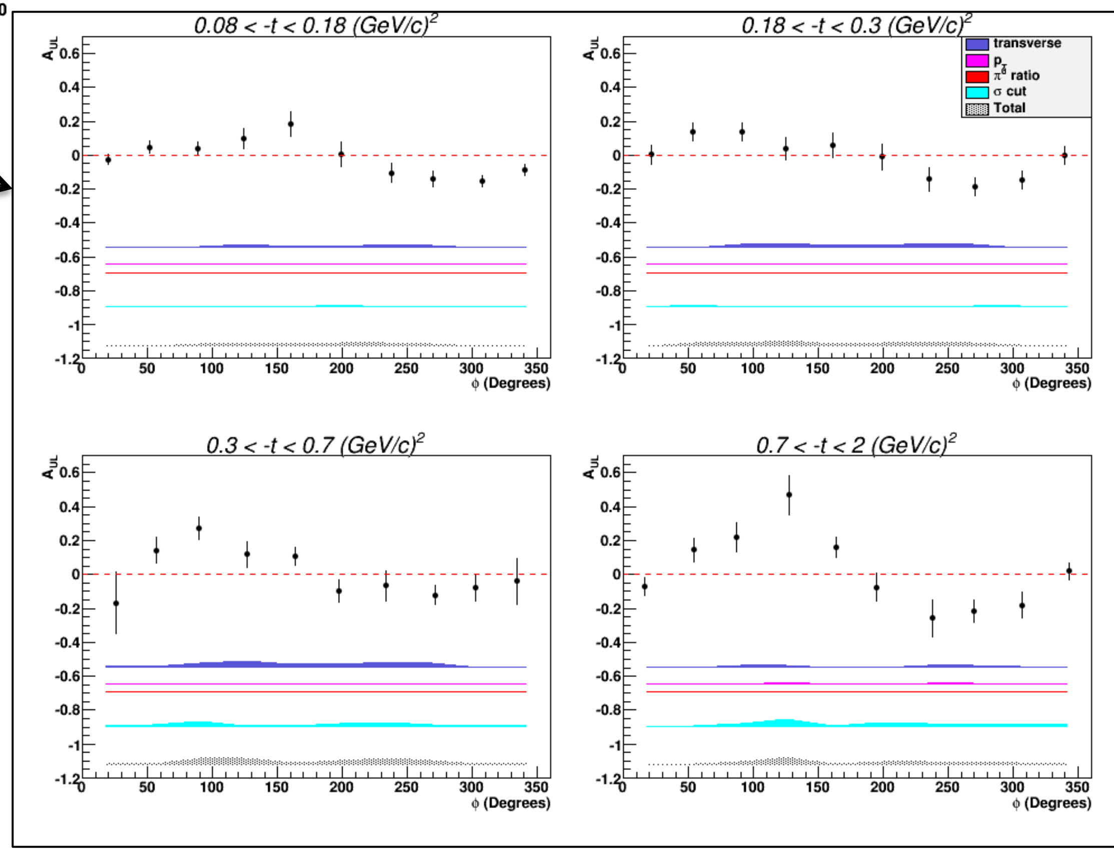

	Source
1	Transverse corrections
2	P_t (P_b)
3	epπ^0 background subtraction
4	DVCS exclusivity cuts

Target-Spin Asymmetry

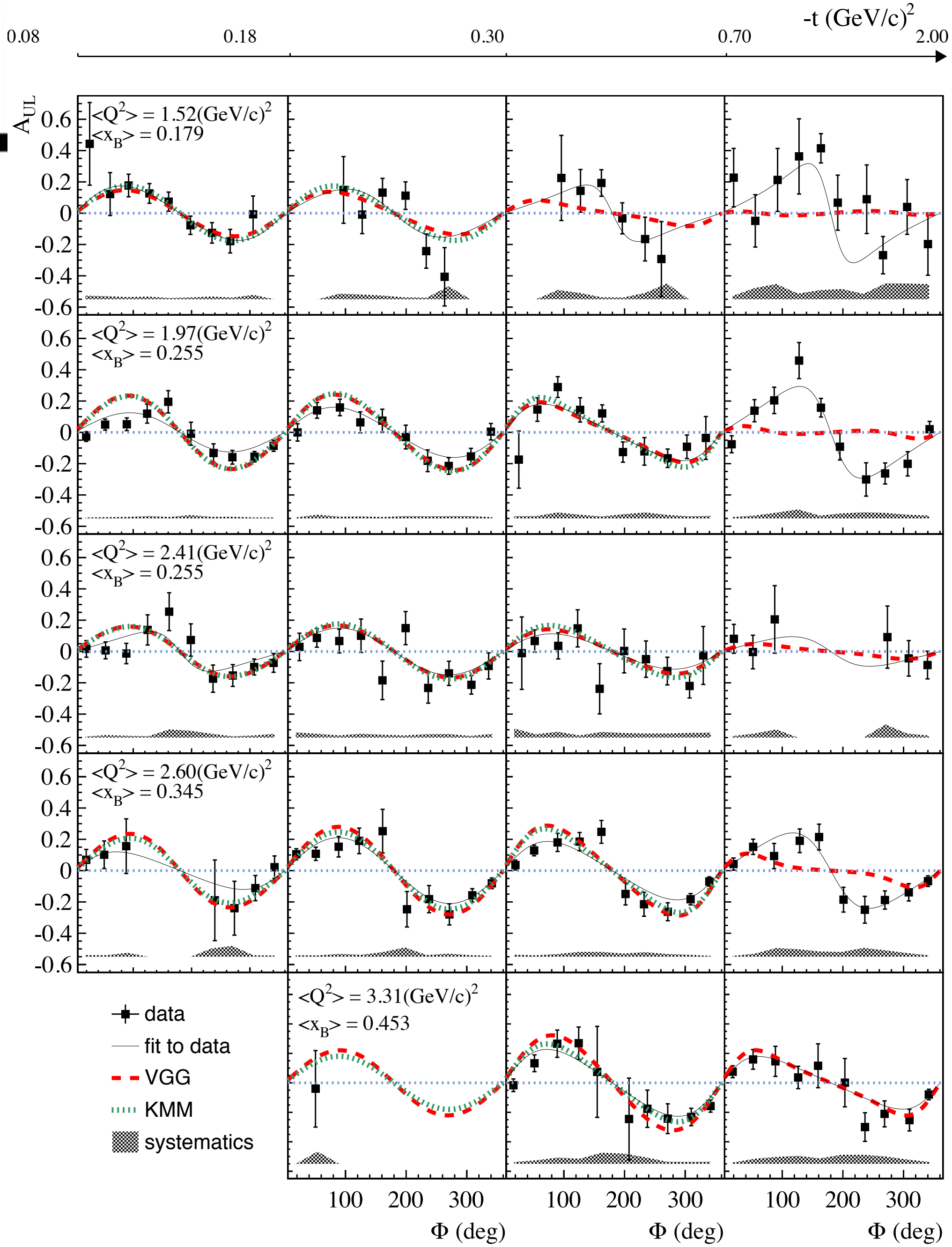

Fit function: $$\frac{\alpha_{UL}\sin(\phi)}{1+\beta\cos(\phi)}$$ $\leftarrow \Delta\sigma$, $\leftarrow \sigma_{total}$

$$Q^2 = -(\mathbf{p}_e - \mathbf{p}_{e'})^2,\ x_B = \frac{Q^2}{2M_p(E_e - E_{e'})}$$

$$t = (\mathbf{p}_p - \mathbf{p}_{p'})^2$$

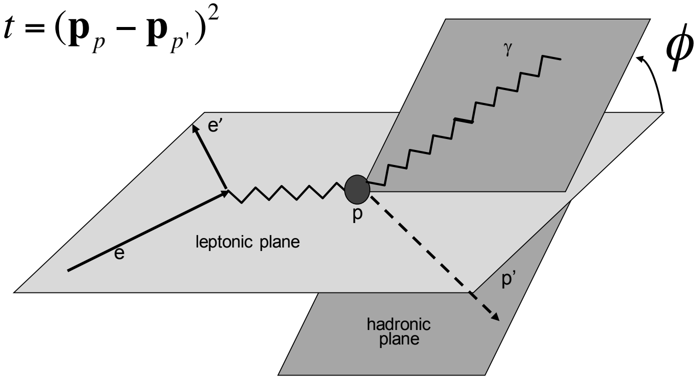

Comparison with Existing World Data

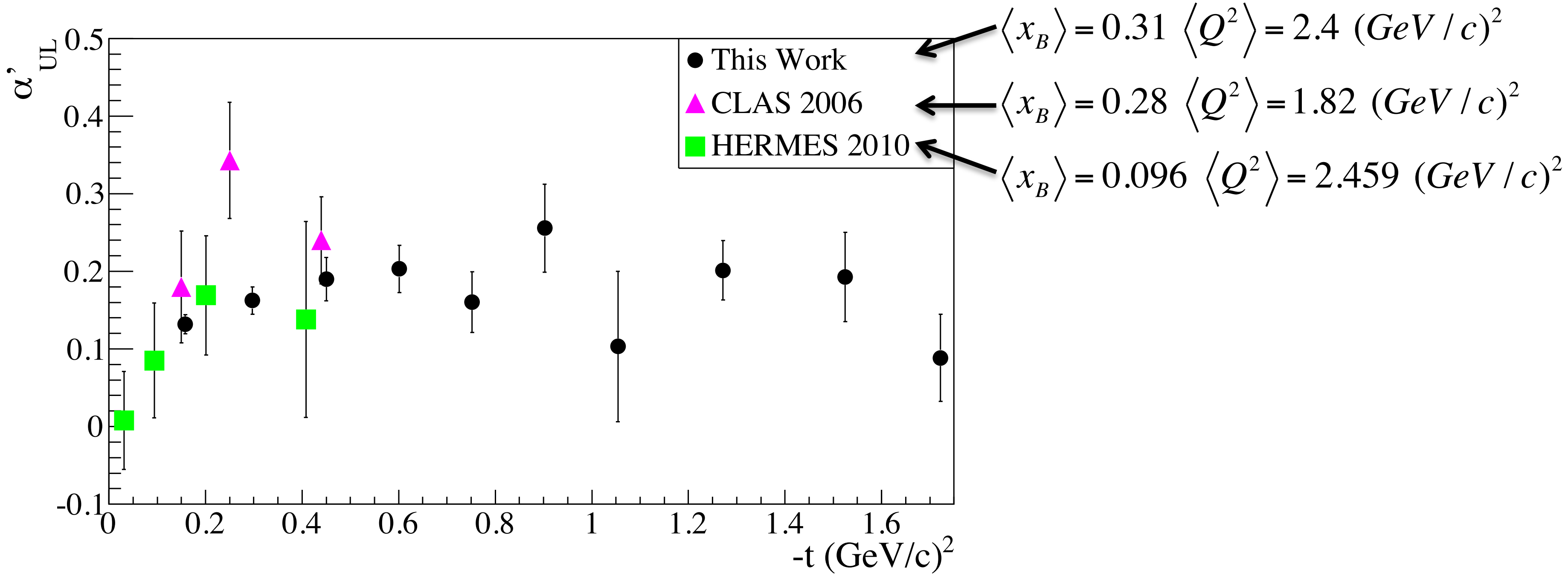

The full 4-D A_{UL} (x_B, Q^2, t, ϕ) measurements are publically available in CLAS Physics Database:

Measurement E139M1

http://clas.sinp.msu.ru/jlab/

$$A_{LU} = \frac{1}{D_f P_b} \frac{(N^{\uparrow\Uparrow} - N^{\downarrow\Uparrow})P^{\Downarrow} + (N^{\uparrow\Downarrow} - N^{\downarrow\Downarrow})P^{\Uparrow}}{(N^{\uparrow\Uparrow} + N^{\downarrow\Uparrow})P^{\Downarrow} + (N^{\uparrow\Downarrow} + N^{\downarrow\Downarrow})P^{\Uparrow}}$$

$$A_{LL} = \frac{1}{D_f P_b} \frac{(N^{\uparrow\Uparrow} + N^{\downarrow\Downarrow}) - (N^{\uparrow\Downarrow} + N^{\downarrow\Uparrow})}{(N^{\downarrow\Uparrow} + N^{\uparrow\Uparrow})P^{\Downarrow} + (N^{\downarrow\Downarrow} + N^{\uparrow\Downarrow})P^{\Uparrow}}$$

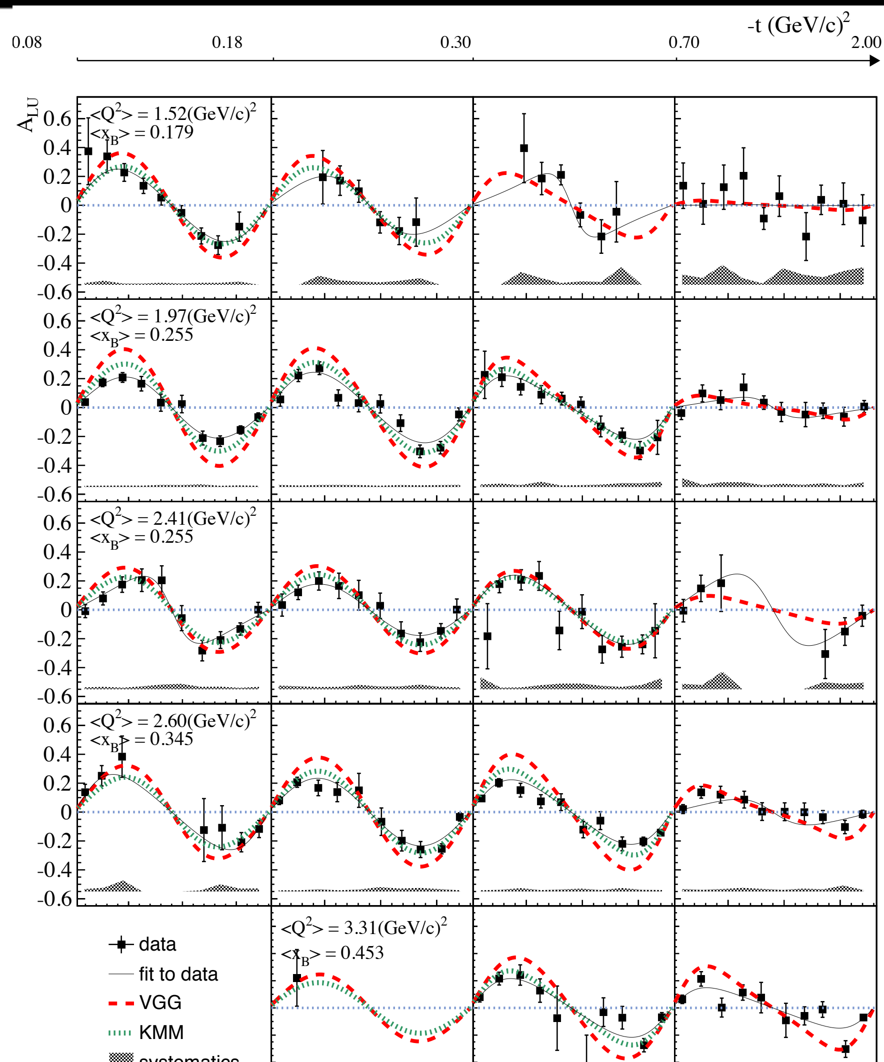

$$\frac{\alpha_{LU}\sin(\phi)}{1+\beta\cos(\phi)}$$

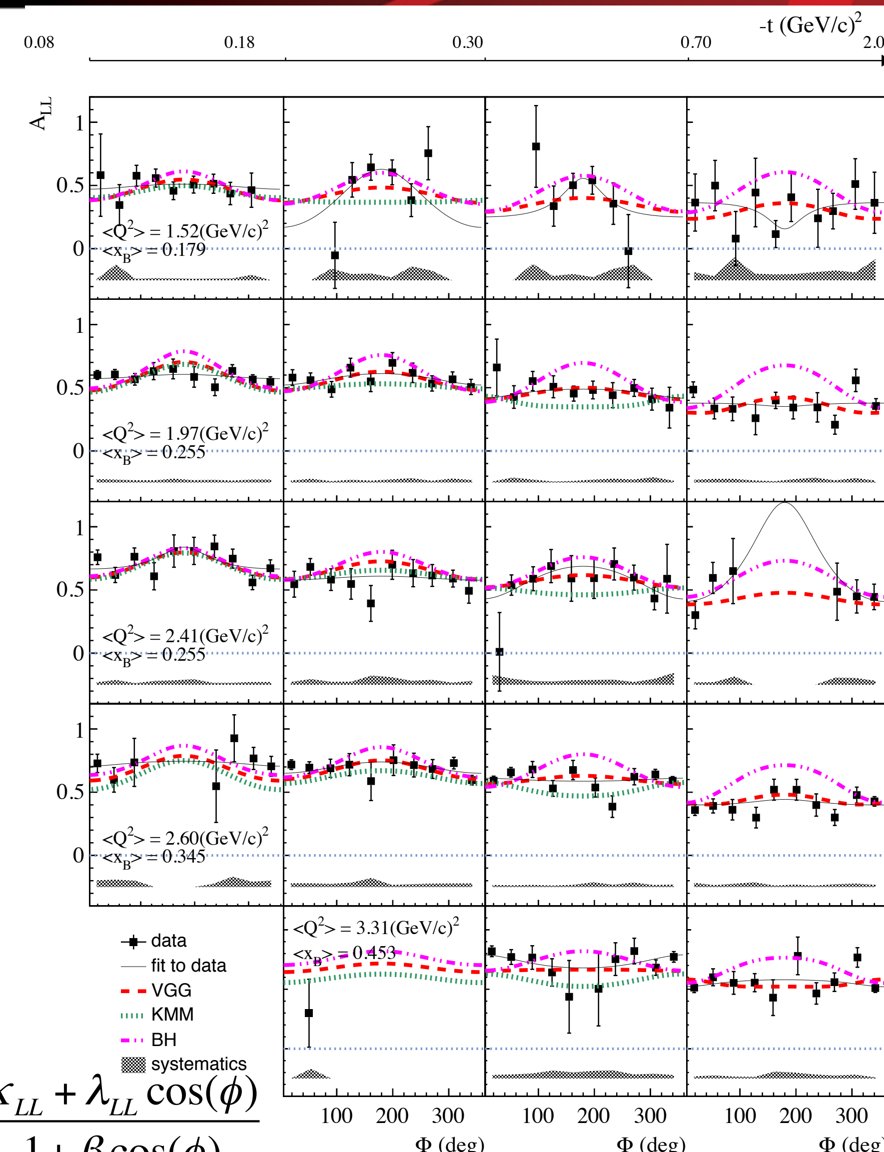

$$\frac{\kappa_{LL} + \lambda_{LL}\cos(\phi)}{1+\beta\cos(\phi)}$$

Beam-Spin Asymmetry

Fit function: $\frac{\alpha_{LU} \sin(\phi)}{1+\beta\cos(\phi)}$

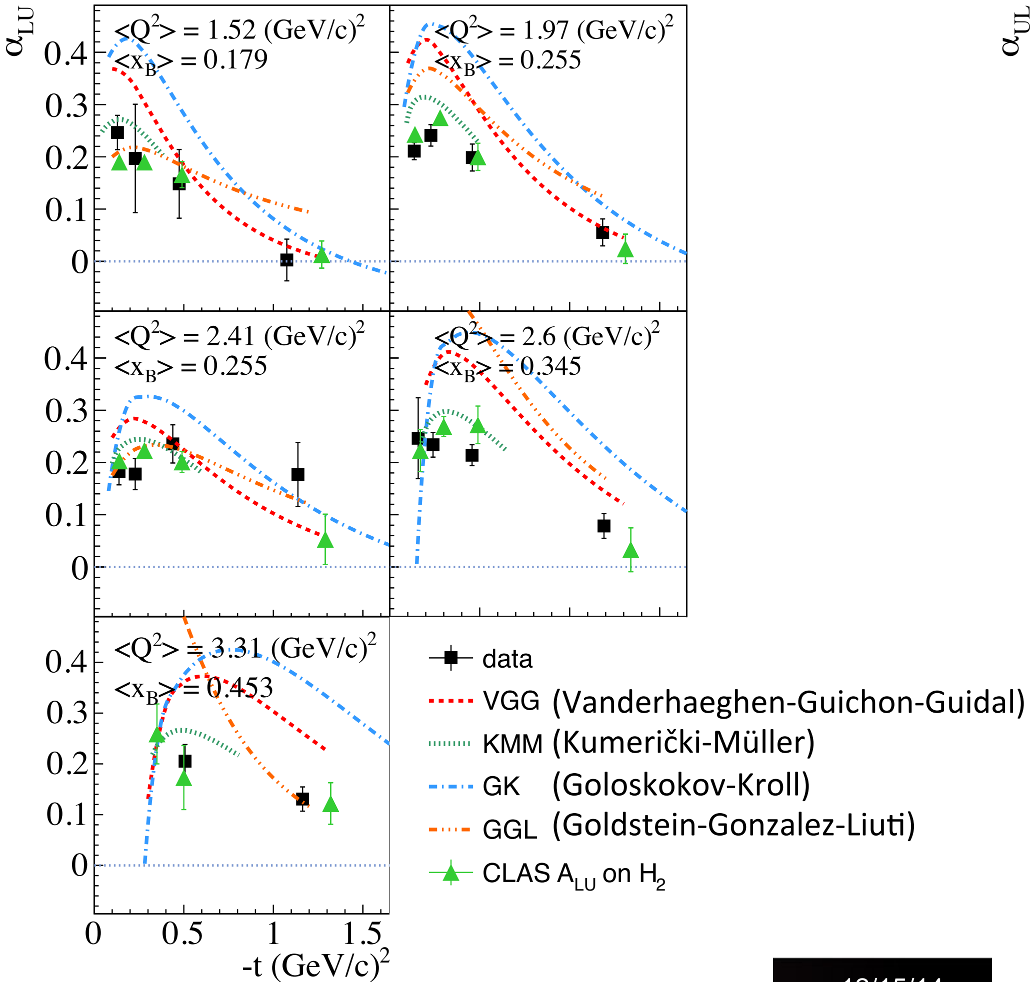

Target-Spin Asymmetry

Fit function: $\frac{\alpha_{UL} \sin(\phi)}{1+\beta\cos(\phi)}$

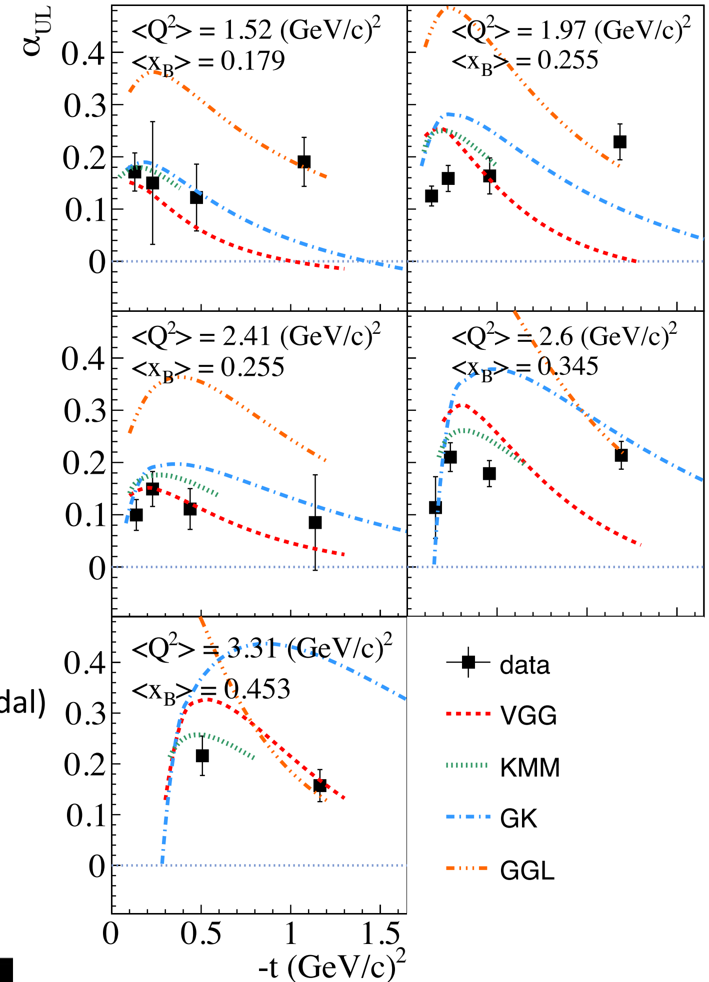

Compton Form Factors (CFFs)

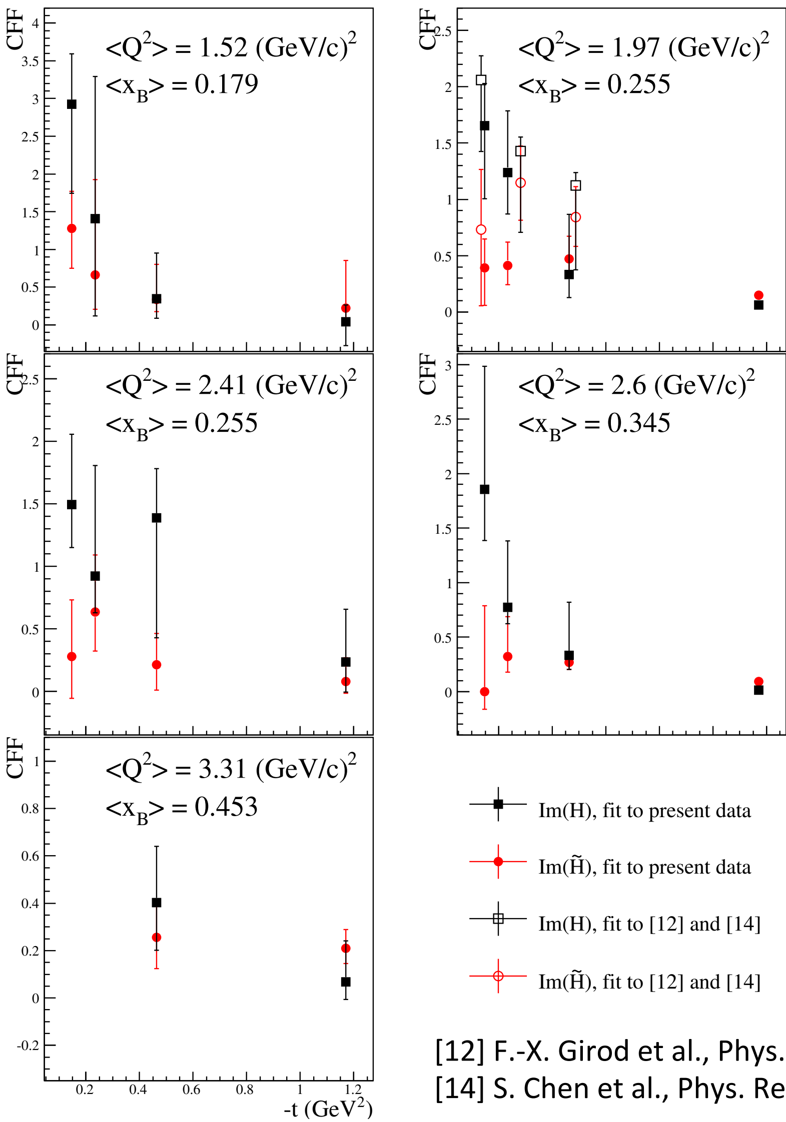

$A_{LU}(x_B, Q^2, t, \phi)$, $A_{UL}(x_B, Q^2, t, \phi)$, and $A_{LL}(x_B, Q^2, t, \phi)$ processed using a fitting procedure :

$\Im m(\tilde{\mathcal{E}})$ set to zero, as $\Im m(\tilde{\mathcal{E}})$ is assumed to be purely real (parametrized, in the VGG model, by the pion pole (1/(t – m2π)))

the values of the real and imaginary parts of the 7 other Compton Form Factors are allowed to vary within ±5 times the values predicted by the VGG model

(t-slope of $\Im m(\mathcal{H})$) > (t-slope of $\Im m(\tilde{\mathcal{H}})$)

hinting that the axial charge (linked to $\Im m(\tilde{\mathcal{H}})$) might be more "concentrated" in the center of the nucleon than the electric charge (linked to $\Im m(\mathcal{H})$).

[12] F.-X. Girod et al., Phys. Rev. Lett. 100, 162002 (2008).
[14] S. Chen et al., Phys. Rev. Lett. 97, 072002 (2006).

Summary

➢ GPDs provide a unique tool to study the internal dynamics of the nucleon.

➢ Their unambiguous extraction from experimental data requires many measurements including DVCS spin observables across large regions of phase space.

➢ The eg1-dvcs experiment was the first DVCS-dedicated longitudinally polarized target experiment performed with the CLAS detector.

➢ The simultaneous presence of a polarized beam and longitudinally polarized target allowed extraction of 3 polarization observables: beam-spin, target- spin and double-spin asymmetries, over a wide Q^2, x_B, and -t phase space.

➢ The measurement of the 3 DVCS observables in the same kinematic regions provides more constraints than previously available for GPD extraction.

➢ The Future: JLab12 GeV and CLAS upgrades increases the available kinematic regions essential for the continuation of the DVCS program for high precision studies of nucleon structure in the valence region.

Proton Polarization

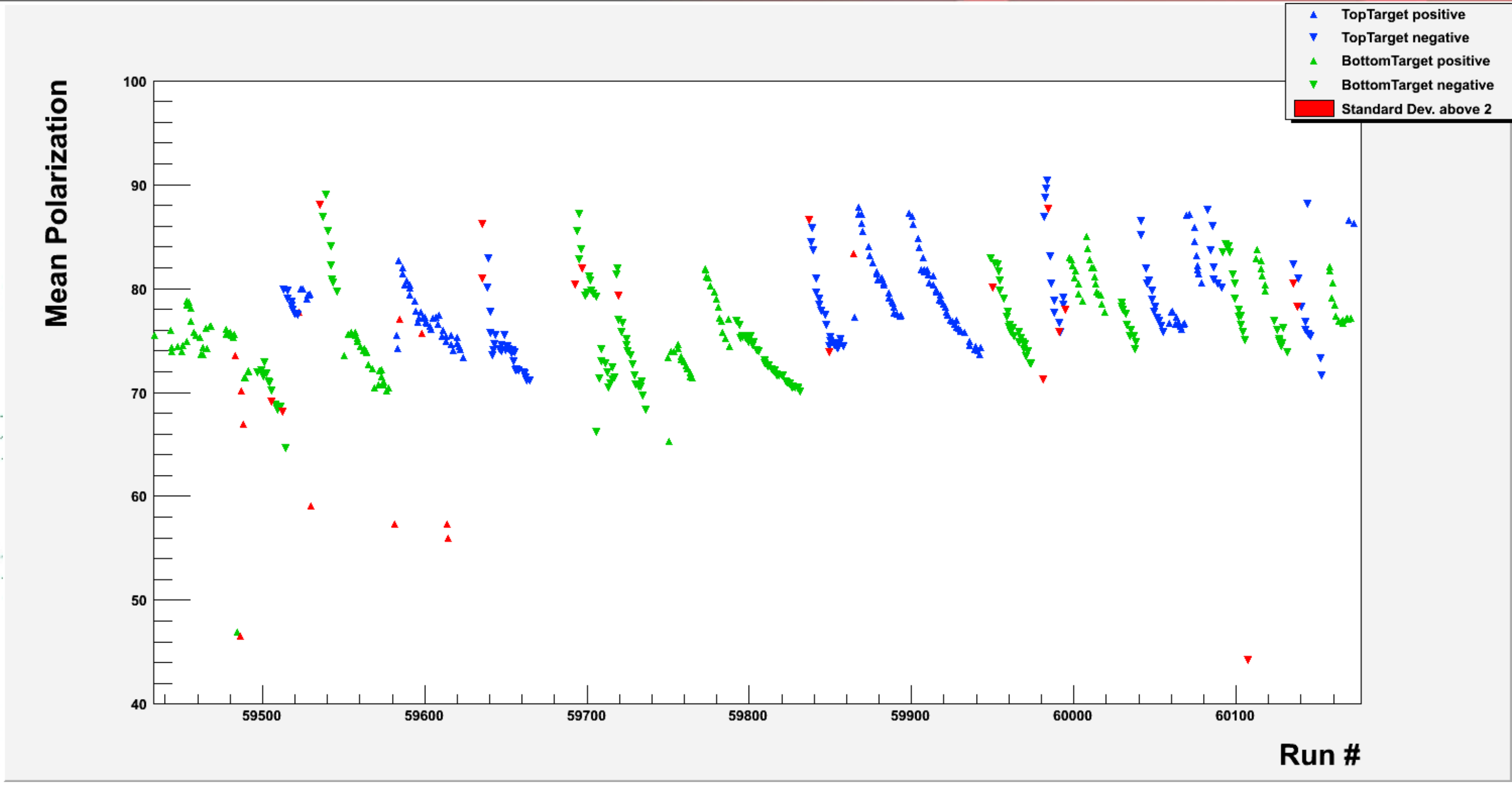

Polarization monitored using proton NMR measurements

- coils wrapped around target cups
- very useful for relative polarization monitoring
- drawback: the target material closest to the coils does not receive beam
  - non-uniformity of the polarization unknown
    - ➔not used for final polarization values